agronomy

MDPI

Article

Molecular Detection of Airborne Sporangia of *Pseudoperonospora humuli* by Quantitative Real-Time PCR and Spore Traps in Czech Hops Production Gardens for Monitoring, Prediction and Disease Management

Markéta Trefilová [1,2,*], Ivo Klapal [1], Alena Henychová [1] and Josef Patzak [1]

[1] Hop Research Institute Co., Ltd., Kadaňská 2525, 438 01 Žatec, Czech Republic; patzak@chizatec.cz (J.P.)
[2] Faculty of Agrobiology, Food and Natural Resources, Czech University of Life Sciences Prague, Kamýcká 129, 165 00 Prague 6, Czech Republic
* Correspondence: trefilova@chizatec.cz

Abstract

Downy mildew of hops represents a serious disease affecting hops production in all growing regions. Disease management is primarily based on the application of fungicides at regular intervals based on a short-term forecasting methodology that is essential for evaluating the occurrence of theoretical infections. To enable a more reliable assessment of the pathogen's presence in a given area, spore traps capturing airborne *Pseudoperonospora humuli* sporangia can be utilized. The use of quantitative real-time PCR (qRT-PCR) for the detection of sporangia collected by these traps allows for the elimination of laborious and time-consuming microscopic counting. Among four tested *P. humuli*-specific nuclear DNA sequences, an effective qRT-PCR detection method was developed based on the c127233.5e3 sequence. This detection approach was used for the quantification of sporangia from volumetric spore trap samples collected in situ under field conditions at three selected localities in Bohemia and Moravia during the 2021–2022 period. The obtained results were compared with the short-term forecasting method of the downy mildew (HDM) weather index (I) based on meteorological data. The overall course of the HDM weather index (I) closely correlated with the occurrence of sporangia: after reaching the maximum HDM weather index (I) value, the highest sporangium detection was observed with a time delay of 1–2 weeks at all the monitored sites. The results corresponded well with data obtained from volumetric spore traps in Germany, and the qRT-PCR method proved to be fully comparable to light microscopy. The combination of volumetric spore traps and qRT-PCR can significantly improve the precision of short-term forecasting systems for *P. humuli* infection, thereby enabling more efficient fungicide application programs in hops protection and contributing to a better understanding of the pathogen's dispersal dynamics.

Keywords: spore detection; *P. humuli*; disease management; hops; qRT-PCR method

Check for updates

Academic Editor: Caterina Morcia

Received: 3 February 2026
Revised: 11 February 2026
Accepted: 12 February 2026
Published: 15 February 2026

Copyright: © 2026 by the authors. Licensee MDPI, Basel, Switzerland. This article is an open access article distributed under the terms and conditions of the Creative Commons Attribution (CC BY) license.

1. Introduction

Hops (*Humulus lupulus* L.) are perennial dioecious plants, grown primarily for their cones, which contain a number of important substances for subsequent processing, especially in beer production, where they have a specific effect on not only the brewing process itself and the bitterness, taste, and quality of the beer [1], but also on the beer's preservation, due to their antimicrobial properties [2]. Another important quality parameter of processed

hops is the content of pesticide residues and heavy metals. Among heavy metals, the most relevant parameter for hops (dried cones) is the copper content. Residues of applied pesticide substances represent a risk not only for hop purchase and trade but, in the case of copper-based fungicides, also for the environment, where it is necessary to regulate the maximum annual application rate of copper.

Hops are cultivated in the Czech Republic (CR) on an area of approximately 4800 hectares, distributed across three hop-growing regions, which are, in descending order of size, Žatec (Saaz), Tršice, and Úštěk regions. From the perspective of global production, the CR ranks third worldwide, following Germany and the United States.

Hops downy mildew (HDM), caused by *P. humuli*, is an obligate biotrophic oomycete responsible for significant yield losses, but more importantly, for the reduction in hop quality. The extent of damage caused by *P. humuli* varies depending on the susceptibility of the cultivar, the timing of infection, and prevailing weather conditions [3]. Due to the higher sensitivity of fructifying organs, late infections occurring during flowering and cone development may cause not only the cessation of growth and cone malformation, but also a reduction in the content of bitter acids, which ultimately has a negative impact on the market value [4]. The development of infection occurs under favorable conditions, primarily determined by the duration of leaf wetness, high relative humidity, and temperature ranging from 8 to 23 °C, depending on the infected part of the plant [4]. The pathogen overwinters as mycelium in infected hop crowns, and during autumn, it infects individual buds from which aerial shoots emerge after pruning in the spring. In cases of severe colonization, the pathogen induces the growth of spike shoots, which serve as a source of primary inoculum and subsequently enable the spread of secondary infection during the growing season.

Protection against *P. humuli* in the CR is based on the integration of direct and indirect control methods. The indirect methods include a set of agronomic and agrotechnical practices, whereas the direct ones rely mainly on the application of fungicides at regular intervals, according to a modified short-term forecasting method [5]. A similar forecasting approach has been tested in the United States for primary infection by *P. humuli* [6] and in Germany for powdery mildew of hops (*Sphaerotheca humuli*) [7]. A major limitation of this method lies in the lack of information on the quantity of inoculum present in the air during different phenological stages. Information about pathogen presence in the crop is derived solely from visual disease symptoms and meteorological data collected during a given season. To address this limitation, volumetric spore traps can be employed [8]. This methodology has been used in Germany since 1984 [9], where monitoring of *P. humuli* zoosporangia is conducted at five stations in the Hallertau region and one station each in the Spalt and Hersbruck regions. In the CR, no current hop protection methodology against *P. humuli* has yet utilized data obtained from volumetric spore traps. The main challenges include data collection, data interpretation, and the large area of individual farms, which necessitates the establishment of a sufficiently dense network of traps to ensure optimal coverage. The application of molecular detection methods for identifying *P. humuli* sporangia captured in spore traps allows for the elimination of time-consuming microscopic counting [10]. Furthermore, advances in molecular techniques and improved knowledge of the pathogen's genomics have enabled further optimization of detection methods [11–13].

The objective of this study was to develop an efficient and accurate method for DNA extraction and detection of *P. humuli* sporangia using quantitative real-time PCR (qRT-PCR) from samples collected in situ with volumetric spore traps under field conditions at selected sites in Bohemia and Moravia during the 2021–2022 growing seasons. The obtained results were compared with the short-term forecasting methodology and fungicide

application schedules, with the aim of evaluating the applicability of volumetric spore traps in forecasting *P. humuli* infections for the optimized and effective use of fungicide treatments in hop protection.

2. Materials and Methods

2.1. Sampling Locality

The experiment was conducted during the 2021 and 2022 growing seasons, from May to August, in hop yards located in Bohemia, in Stekník (50.3217936 N, 13.6293542 E) and Nesuchyně (50.1726639 N, 13.7006050 E). Both hop yards were planted with the Saaz cultivar and cultivated under conventional management practices. Monitoring was also carried out in Moravia, at Tršice (49.528822 N, 17.429049 E), in a hop yard planted with the Saaz cultivar and managed conventionally. The Saaz cultivar occupies the largest growing area in the CR and is regarded as one of the most susceptible cultivars to *P. humuli* infection, making it an ideal model for studying infection dynamics and the efficacy of control measures. The observed hop yards were treated throughout the vegetation period according to standard cultivation practices, with fungicide selection and timing determined by the grower. The assessment of disease severity was carried out according to the EPPO standard PP1/003(4) [14]. In spring, excess shoots were mechanically removed during the secondary training stage as part of routine spring operations. These shoots, if heavily colonized, may show the first symptoms of infection, and their removal reduces the amount of primary inoculum of *P. humuli*. Since all monitored hop yards were planted with the same cultivar, the timing of protective treatments was similar among sites, with minor differences mainly due to variations in the timing of spring pruning, which influenced the stage of plant growth.

2.2. Air Samplers

Airborne inoculum was collected using a seven-day automatic volumetric spore trap (AMET, Velké Bílovice, Czech Republic) based on the Hirst principle [8]. The traps were operated continuously from 8 May to 23 August 2021 and from 1 May to 31 August 2022. They were installed on the leeward side of hop yards, near untreated plots, and were not protected from precipitation. To avoid interference with field machinery, the traps were anchored near hop poles. The air intake of the trap was positioned 1.5 m above the soil surface. As a sampling medium, a Melinex tape (Mylar Specialty Films, DuPont Teijin Films UK Ltd., Middlesbrough, UK) coated with petroleum jelly was used, mounted on the rotating drum of the sampler. The airflow rate was maintained at a constant 10 L min^{-1}. Samples, i.e., the tapes, were collected at regular seven-day intervals. In the laboratory, the obtained tapes were cut with sterile scissors into segments corresponding to individual days (a 24 h collection period represented 48 mm of tape) and stored in 2 mL microtubes at −20 °C until further analysis.

2.3. Meteorological Data

Meteorological data were recorded using automatic weather stations (Smart Hop Garden, Ing. Radovan Breuss, Dolní Břežany, Czech Republic) located either directly within the monitored hop yards or within a distance of up to 1 km. These stations characterize the microclimate of a specific area or district and serve as a basis for forecasting and signaling spray applications within a 10 km radius of hop gardens. Data obtained from the selected stations included daily mean air temperature (t), daily mean relative air humidity (R), and daily precipitation amount (r).

These parameters constitute a simplified model of the hop yard climate and were used to calculate the "small index" of downy mildew weather according to the following formulas:

For days with precipitation:

$$i = 100 + 10\ x\ (t - 15) + 2\ x\ (R - 60) + r \quad (1)$$

For days without precipitation:

$$i = \frac{100 + 10\ x\ (t - 15) + 2\ x\ (R - 60)}{S} \quad (2)$$

where i = "small" index of downy mildew weather; t = mean daily air temperature (°C); R = mean daily relative air humidity (%); r = daily precipitation total (mm, rounded to whole millimeters); S = number of rainless days (length of the dry period) (1) (2). For evaluation purposes, a "large index" (I) was calculated, representing the five-day sum of the small index values [5].

2.4. DNA Extraction

Genomic DNA was isolated from Melinex tape samples using DNeasy Plant Mini Kit (Qiagen, Hilden, Germany) according to Hospodsky et al. [15]. Twenty pieces of 2 mm glass beads (SigmaAldrich, Merck Life Science, Prague, Czech Republic), 400 µL of AP1 buffer, and 4 µL of RNase were added to the Eppendorf microtube of each day's Melinex tape samples. The samples were homogenized by mixing two times for 60 s on a high-speed (30 Hz) homogenizer FastPrep 24 (MP Biomedicals, LLC, Solon, OH, USA). After that, the samples were incubated at 65 °C for 10 min with three times mixing by inverting, and DNA isolation continued according to the producer's protocol. DNA was eluted from the column by 100 µL of sterile ddH_2O and stored at −20 °C until analysis. For absolute sporangium quantification, leaves from infected hop basal spikes were suspended in 100 mL of distilled water to make a sporangium suspension. Sporangium concentration was counted in a Bürker chamber under a light microscope. Single-day Melinex tape parts were spiked with 10, 20, 50, 100, or 300 sporangia for statistical analysis. An EZNA Fungal DNA Mini Kit (Omega Biotek, Norcross, GA, USA) was used for DNA isolation from the sporangium suspension, concentrated by centrifugation, for quantification.

A DNA mixture of all *P. humuli* isolates from our previous work [16] was used as the internal positive control. DNA from sterile in vitro hop plants was used as the extraction negative control. DNA concentrations were quantified by measuring UV absorbance at 260 nm on a UV-VIS spectrophotometer (UV-1601, Shimadzu, Kyoto, Japan).

2.5. Quantitative Real-Time PCR Analyses (qRT-PCR)

RealTime Design software (LGC Biosearch Technologies, Petaluma, CA, USA) was used to design real-time PCR primers (Table 1). Specific PCR primers and internal BHQ1 probes were designed based on the ITS1 region of the rDNA sequence (qDMITS1-110 bp PCR product) according to Werschallova et al. [16] and sequences c127446.1e1 (qPhu1-72 bp PCR product), c127233.5e3 (qPhu2-74 bp PCR product), and c126365.1e5 (qPhu3-98 bp PCR product) according to Rahman et al. [17], and synthesized by Generi-Biotech (Hradec Kralove, Czech Republic). As the ITS1 region is much conserved and species-specific, we carried out a sequence multi-alignment comparison of the closest fungal species [16,18,19] using Geneious Pro 4.8.2 (Biomatters Ltd., Auckland, New Zealand) [16]. The following isolates were used: *P. humuli* HDM263 (JF304685), *P. cubensis* CDM248 (JF304657), *P. celtidis* SMK17780 (JF314768), *P. cannabina* MZM71018 (AY608612), *P. urticae* HOH1111 (HM636048), *Peronospora arborescens* P9ELE (DQ885366), *Peronospora destructor* PD1 (OR365096), and

Peronospora sparsa SMK17872 (DQ874344). The sequence multi-alignment comparison with primers and internal BHQ1 probe localization is shown in Figure 1.

Table 1. Nucleotide sequences of specific primers for qRT-PCR.

Primer	Forward Primer (5′→3′)	Reverse Primer (3′→5′)
qDMITS1	TACTGCTAGGCGAGCCCTAT	GAGACTTTCGTCCCCACAGT
qPhu1	GGAGGTGTGGGTGAAGTCTA	CGTCGCATGGTTCGTTGATG
qPhu2	TCGTGAGCACATCGAGAAAC	GCGTGAGACCGTTACCAA
qPhu3	CTTGCGCTTGAGTTGCTACTTC	
Probe	**Probe (5′→3′)**	
qDMITS1probe	AGCGTTTGGGCTTCGGTCTGAAC	AAGCTCGTGGTCAGGATGA
qPhu2 probe	TCCGACTGTACGTGCTGATCACA	

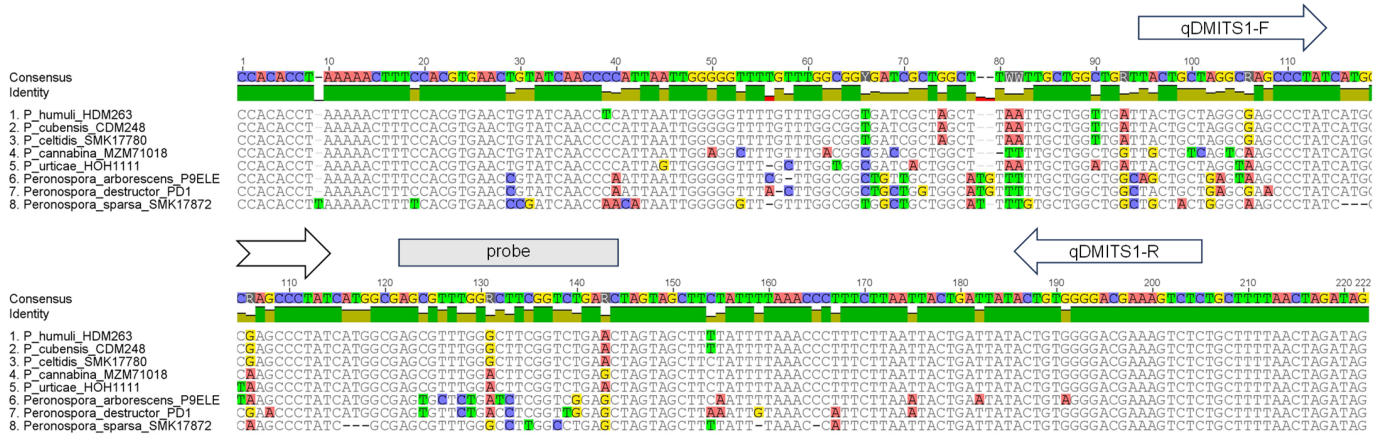


Figure 1. Sequence multi-alignment comparison of eight species-specific ITS1 region sequences with primers (arrows) and internal BHQ1 probe (rectangle) localization. The colored nucleotides among the sequence represent disagreements with the consensus sequence.

Other specific primers and probe sequences were compared to known nucleotide sequences in GeneBank https://www.ncbi.nlm.nih.gov/genbank/ (accessed on 30 December 2025), using Nucleotide BLAST (Bethesda, MD, USA) https://blast.ncbi.nlm.nih.gov/Blast.cgi (accessed on 30 December 2025) to determine their homology. The maximum homology found for all sequences was 95%, when the forward and reverse primers and probe were always located on different DNA sequences.

In total, 2 µL of DNA sample and 300 nM of specific primers were used for a 20 µL PCR reaction with 10 µL of iTaq universal SYBR green supermix or iTaq universal probes supermix (Bio-Rad Laboratories, Hercules, CA, USA) with the addition of 200 nM of specific probe. All amplifications were carried out in technical duplicates on a Real-time PCR cycler CFX Connect (Bio-Rad Laboratories, Hercules, CA, USA), starting with an initial denaturation/Taq activation step (95 °C for 10 min), followed by PCR for 45 cycles (94 °C for 15 s, 59–60 °C for 25 s, and 72 °C for 20 s) and melting curve analysis (from 65 °C to 95 °C). Every run included standard calibration curve samples, internal positive control, extraction negative control, and reactive (sterile ddH_2O) negative control according to the EPPO Standard PM 7/98 [20].

2.6. Statistical Analyses

The standard calibration curves for *P. humuli* DNA concentration and sporangium quantification were generated using singleplex reactions of the studied primer pairs with 5-fold dilution series in triplicate according to the EPPO Standard PM 7/98 [20]. qRT-PCR efficiencies were calculated using Bio-Rad CFX Manager software (Bio-Rad Laboratories,

Hercules, CA, USA). Logarithmic equations of individual standard calibration curves were calculated based on the obtained data. For the lowest detected DNA concentrations and numbers of sporangia, qRT-PCR assays of the studied primer pairs were performed in ten replicates. The Limit of Detection (LOD) and Limit of Quantification (LOQ) were calculated according to the following formulas:

$$\mathbf{LOD} = \frac{\mathbf{3.3\ x\ SD}}{\mathbf{Slope}} \quad (3)$$

$$\mathbf{LOQ} = \frac{\mathbf{10\ x\ SD}}{\mathbf{Slope}} \quad (4)$$

Three technical replicates of four independent extractions of each sporangium dilution on Melinex tape were used for regression analysis. For further regression analysis, 1 ng of positive internal DNA control was added to the reaction mixture for four samples of independent extractions. The obtained qPhu2 equations were used for the calculation of sporangia trapped on Melinex tape samples. All statistical analyses and plots were visualized using Microsoft Excel (Microsoft Office 2016, Microsoft Corporation, Redmond, WA, USA).

3. Results

3.1. Evaluation of Sensitivity and Specificity of qRT-PCR

3.1.1. Analytical Specificity of the qRT-PCR Assay

The specificity of the qRT-PCR assay of all four primer combinations was tested on all *P. humuli* isolates from our previous work [16]. The PCR products were amplified for all isolates. To exclude possible amplification in non-target organisms, the primer combinations were tested on DNA from other fungal pathogens occurring on hops [21]. All samples were negative in the qRT-PCR tests.

Unfortunately, species specificity was not observed for the qDMITS1 primer combination, as the sequences are identical for *P. humuli*, *P. cubensis*, and *P. celtidis* (Figure 1). However, it differs from the other two species, *P. cannabina* and *P. urticae*. This primer combination can only be used as a control and for testing infection in plants where other *Pseudoperonospora* species do not occur. The specificity of the qRT-PCR assay for the other three primer combinations was guaranteed by using unique primer sequences from the *P. humuli* genome without any absolute homology with *P. cubensis* or other fungal species.

3.1.2. Analytical Sensitivity and Amplification Efficiency of qRT-PCR Primers

The analytical sensitivity of the four designed primer pairs was evaluated by standard curves using a 5-fold dilution series for quantified positive internal control DNA concentrations from 100 fg to 10 ng and quantified sporangium concentrations from 2.5 to 500 sporangia in triplicate. The results are shown in Figures 2 and 3. The qDMITS1 primer pair was the most amplified due to the multicopy of the rDNA sequence in the *P. humuli* genome. The qRT-PCR assay exhibited a significant linear logarithmic response with an efficiency of 115% (R^2 = 0.9743 and 0.9901). The amplification of the qPhu2 primer pair was lower but still more effective than both qPhu1 and qPhu3. The PCR efficiencies were 92% (R^2 = 0.9691 and 0.9734), 97% (R^2 = 0.9842 and 0.9863), and 99% (R^2 = 0.9668 and 0.9632) for qPhu1, qPhu2, and qPhu3, respectively. Melting curve analyses confirmed the amplification of the single PCR product for each primer pair, except for qPhu1. The qDMITS1 and qPhu2 primer pairs were selected for testing the internal BHQ1 probes to enhance sequence specificity. Both primer pairs were evaluated by standard curves using a 5-fold dilution series for quantified sporangium concentrations from 0.5 to 250 in triplicate. The internal BHQ1 probes increased the number of PCR cycles for sporangium

quantification for both primer pairs (Figure 4). The PCR efficiencies were 115% (R^2 = 0.9714) and 117% (R^2 = 0.9759) for qDMITS1 and qPhu2 without probes, and 110% (R^2 = 0.9877) and 130% (R^2 = 0.9906) for qDMITS1* and qPhu2* with probes, respectively.

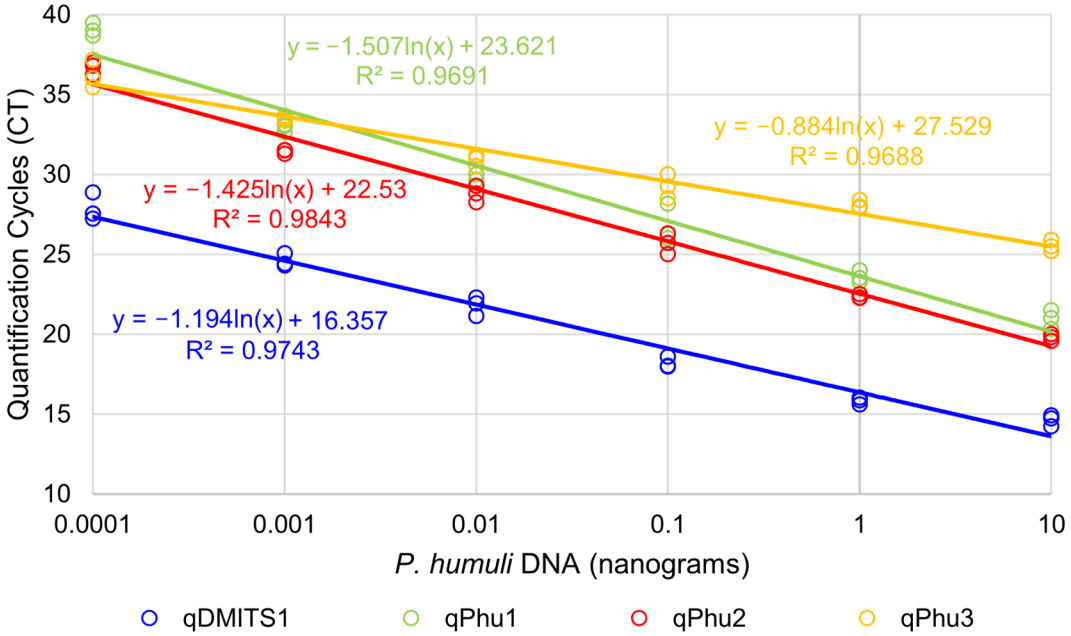


Figure 2. Standard curves for quantification of DNA concentration using qRT-PCR assays based on four specific primer combinations: qDMITS1, qPhu1, qPhu2 and qPhu3. Circles represent individual data for each triplicate. The linear correlation with a regression coefficient (R^2) is presented for each standard curve.

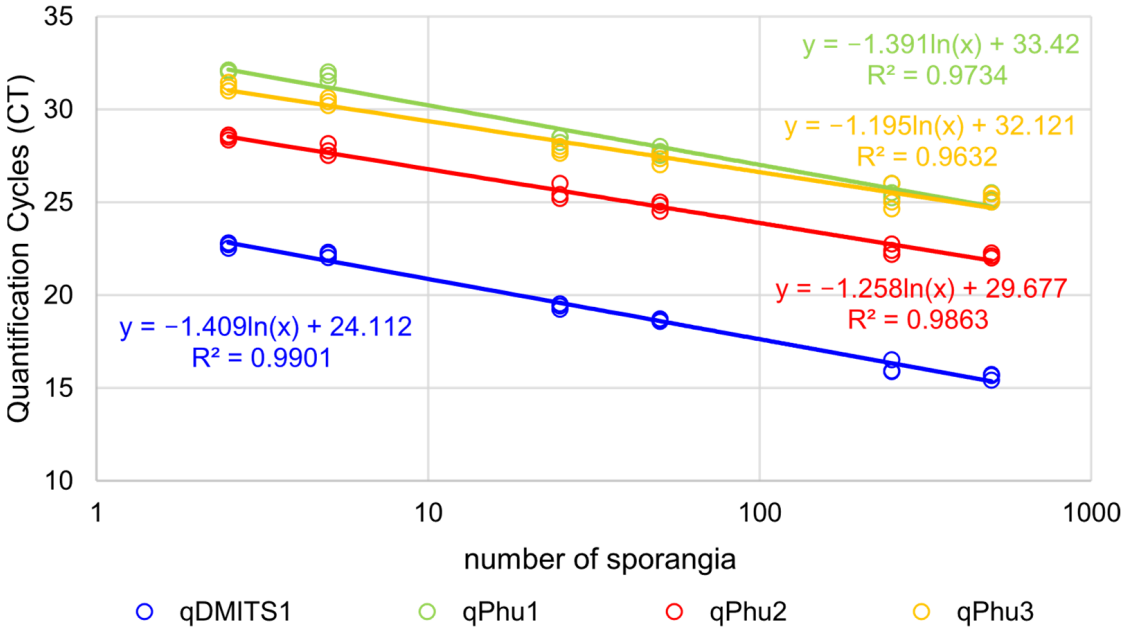


Figure 3. Standard curves for quantification of sporangia using qRT-PCR assays based on four specific primer combination qDMITS1, qPhu1, qPhu2 and qPhu3. Circles represent individual data for each triplicate. The linear correlation with a regression coefficient (R^2) is presented for each standard curve.

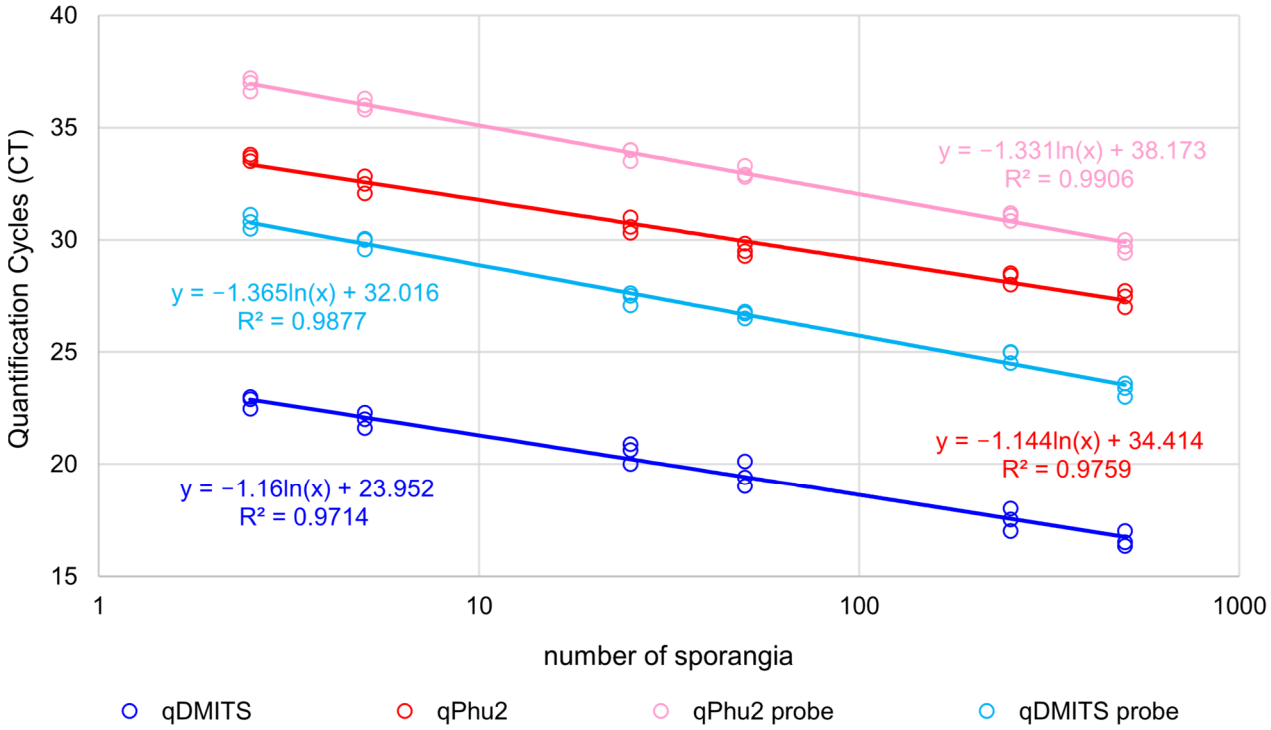


Figure 4. Standard curves for quantification of sporangia using qRT-PCR assays based on two specific primer combinations, qDMITS1 and qPhu2, with SYBR green or internal BHQ1probes qDMITS1* and qPhu2*, respectively. Circles represent individual data for each triplicate. The linear correlation with a regression coefficient (R^2) is presented for each standard curve.

3.1.3. Validation and Analytical Performance of qRT-PCR Assays for Detection of *P. humuli* Sporangia

To determine the minimum analytical sensitivity of the four designed primer pairs and the two internal BHQ1 probes, qRT-PCR assays were run in ten replicates for the lowest detected DNA concentrations and number of sporangia. Based on these results, Limits of Detection (LOD) and Quantification (LOQ) were calculated and are summarized in Table 2.

Table 2. Limit of Detection (LOD) and Limit of Quantification (LOQ) values for four specific primer combinations and two internal BHQ1 probes.

Primer Combination	**qDMITS1**	**qPhu1**	**qPhu2**	**qPhu3**
LOD (fg DNA)	65	75.518	48.499	164
LOQ (fg DNA)	197	228.844	146.967	497
LOD (number of sporangia)	1.487	1.224	1.0684	1.736
LOQ (number of sporangia)	4.507	3.709	3.237	5.260
Primer combination	**qDMITS1**	**qDMITS1 probe**	**qPhu2**	**qPhu2 probe**
LOD (number of sporangia)	1.032	0.9815	1.130	0.705
LOQ (number of sporangia)	3.127	2.9735	3.424	2.135

The lowest minimum sensitivities for internal BHQ1 probes were achieved when the Limits of Detection for the number of sporangia were LOD = 0.705 for qPhu2* and

LOD = 0.9815 for qDMITS1*. The Limits of Quantification for the number of sporangia were LOQ = 2.135 for qPhu2* and LOQ = 2.9735 for qDMITS1*. These two primer pairs also achieved the best results without the internal BHQ1 probes, with qPhu2 being the most sensitive (Table 2).

Samples of spiked Melinex tape with 10, 20, 50, 100, or 300 sporangia were used to prove the best detection capability of trapped airborne sporangia using a qRT-PCR assay with internal BHQ1 probes. The regression analysis confirmed that both primer pairs and internal BHQ1 probes were useful for the quantification of airborne sporangia (Figure 5). The qPhu2* qRT-PCR assay achieved slightly higher correlation (R^2 = 0.7958) than the qDMITS1* qRT-PCR assay (R^2 = 0.7667) and was used for monitoring airborne sporangia using spore traps, also due to its specificity only to *P. humuli* sporangia.

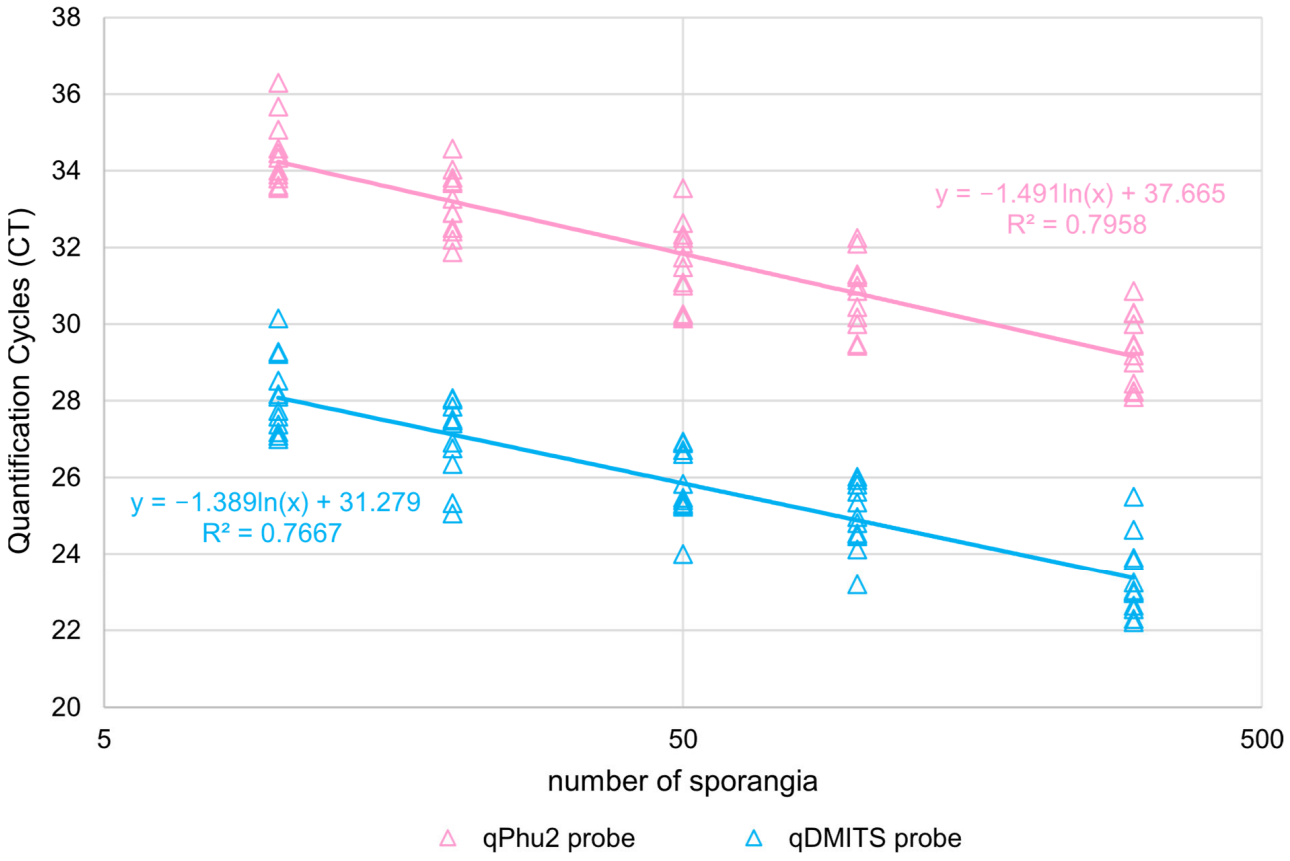


Figure 5. Regression analyses for quantification of sporangium dilution on Melinex tape using qRT-PCR assays based on two specific primer combinations, qDMITS1 and qPhu2, with internal BHQ1probes qDMITS1* and qPhu2*, respectively. Triangles represent individual data for four samples in triplicate. The linear correlation with a regression coefficient (R^2) is presented for each standard curve.

To further verify repeatability and reproducibility, 1 ng of positive internal control DNA was added to the reaction mixture of four independent extraction samples, and regression analysis was performed for the qPhu2* qPCR assay with the internal BHQ1 probe (Figure 6). The analysis confirmed that this qPCR assay is not inhibited by DNA extraction and is reliable for monitoring aerial sporangia using spore traps.

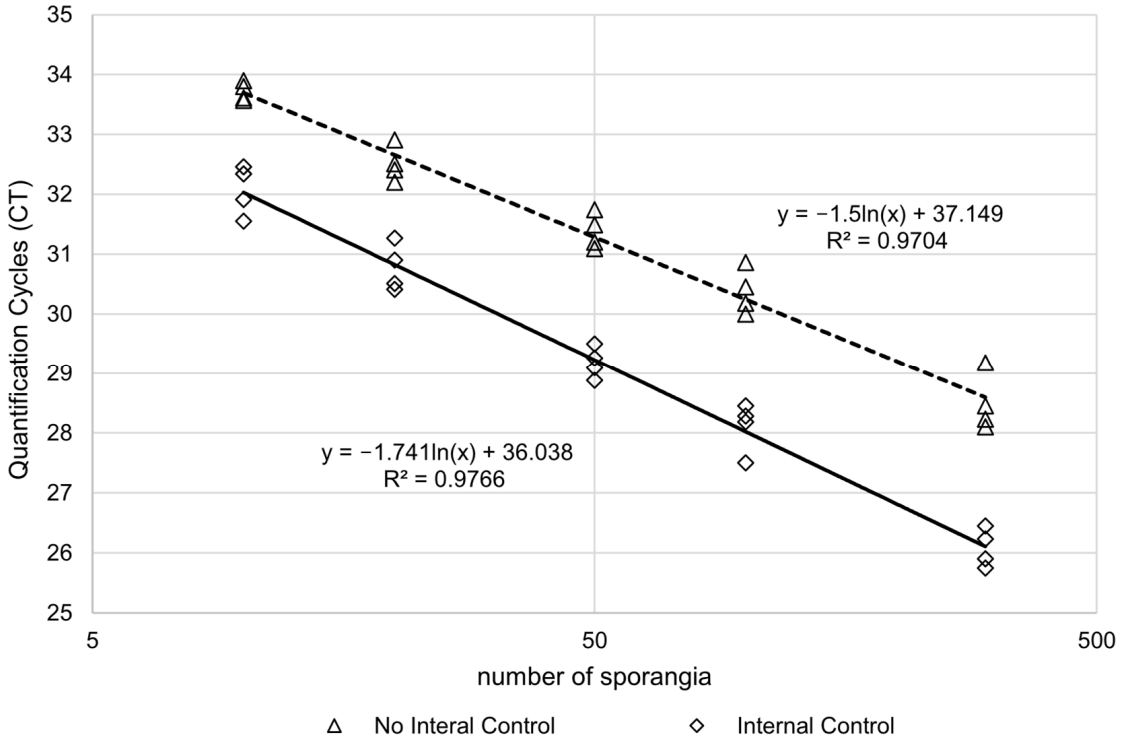


Figure 6. Regression analyses for quantification of sporangium dilution on Melinex tape using qRT-PCR assays based on qPhu2 primer combination with internal BHQ1probe qPhu2* and without (triangles) or with (rhombs) positive internal DNA control. Triangles and rhombs represent individual data for four samples. The linear correlation with a regression coefficient (R^2) is presented for each standard curve.

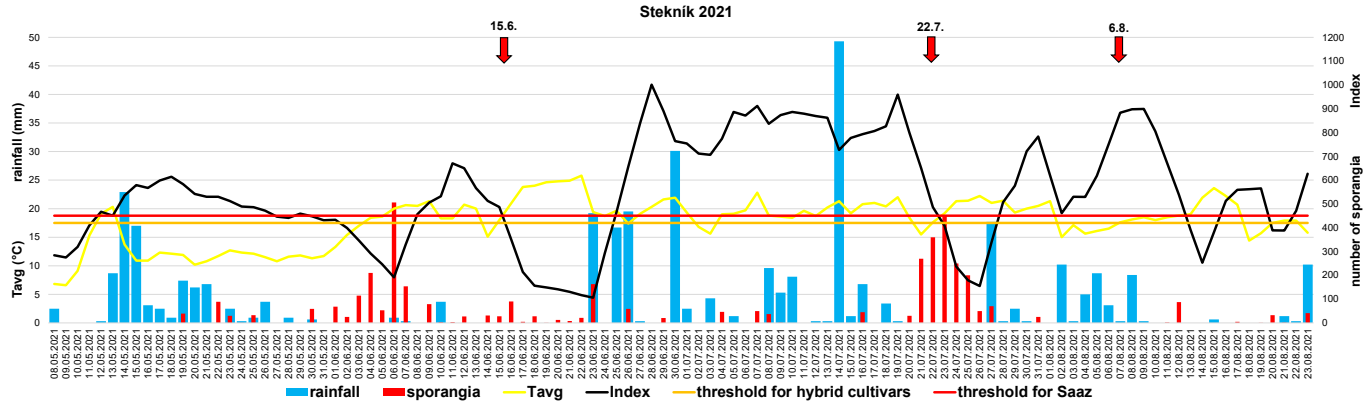
3.2. Monitoring of P. humuli Airborne Sporangia Using Spore Traps and qRT-PCR for Prediction and Disease Management

During the 2020 and 2021 seasons, a total of 672 samples collected between May and August were analyzed by qPCR from three locations in the CR: Stekník and Nesuchyně in Bohemia, and Tršice in Moravia. In 2021, sampling was conducted from 8 May to 23 August, while in 2022 it was carried out from 1 May to 31 August.

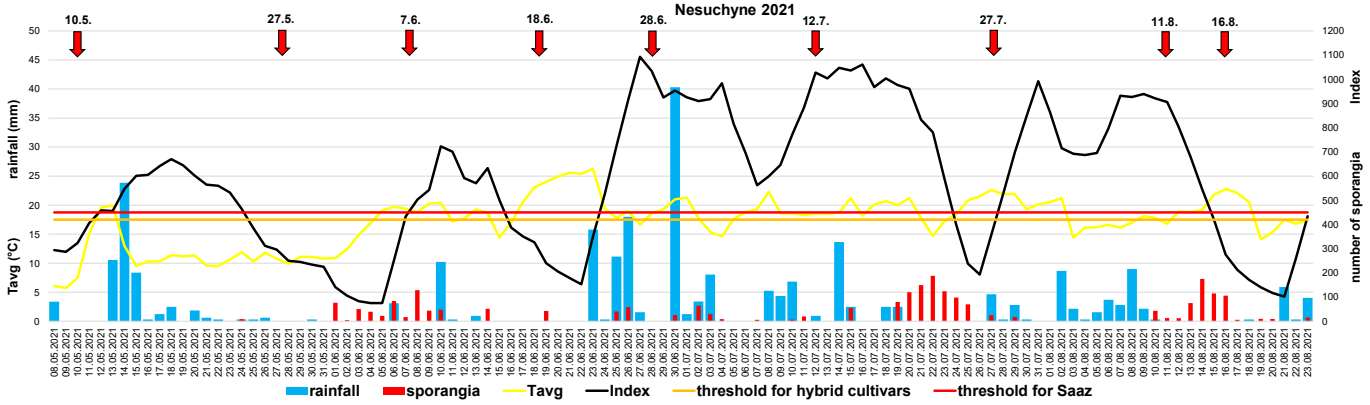
3.2.1. Airborne *P. humuli* Sporangia Occurrence During the 2021 Growing Season

Using qPCR, *P. humuli* sporangia were detected for the first time in commercial hop fields during May 2021 (Stekník, 27 May; Nesuchyně, 24 May; and Tršice, 17 May) (Figure 7a–c). Subsequently, *P. humuli* sporangia were detected almost daily at all monitored sites. The concentration of airborne sporangia at Stekník (Figure 7a) and Nesuchyně (Figure 7b) increased markedly during the first and second weeks of June, with the highest concentrations recorded on June 6 at Stekník and on June 8 at Nesuchyně. At Tršice (Figure 7c), sporangia were first detected during the second week of June, reaching a maximum on 7 June. The overall number of detected sporangia at this site was considerably lower compared to the other locations. *P. humuli* sporangia were subsequently detected during the second and third weeks of June at all sites, with continuous detection at Stekník (Figure 7a), whereas detection at Nesuchyně (Figure 7b) and Tršice (Figure 7c) was sporadic. Peak occurrence was observed at all locations during the fourth week of June. In the first week of July, detection in Bohemia was limited. The second peak of *P. humuli* sporangium occurrence was recorded during the third and fourth weeks of July, both at Stekník, where it culminated on 23 July, and at Nesuchyně, where the highest detection was observed on 22 July. In contrast, at Tršice, the second period of maximum sporangium detection occurred earlier, during the first and second weeks of July, reaching its peak on 6 July. No

P. humuli sporangia were detected during the third week, but they reappeared during the fourth week of July. At the end of the growing season, in the first week of August, *P. humuli* sporangia were not detected at the Stekník (Figure 7a) or Nesuchyně (Figure 7b) sites. At Stekník, detections were sporadic towards the end of the vegetation period, occurring on 12, 17, 20, and 23 August. At Nesuchyně, a third significant wave of sporangium detection was recorded at the transition between the second and third weeks of August, peaking on 14 August. This wave coincided with severe infection symptoms during the cone maturation period. At Tršice (Figure 7c), the most significant sporangium detection occurred in the first week of August, peaking on 7 August, with only sporadic detections thereafter, on 14 August. The HDM weather index (I) fluctuated according to meteorological conditions, reaching the highest values following rainy periods. The overall trend in the HDM weather index (I) closely corresponded to the occurrence of sporangia, with the highest sporangium levels typically observed 1–2 weeks after the HDM weather index (I) reached its maximum at all monitored sites. Fungicide treatments in 2021 were applied by growers at the recommended times according to issued warning signals (Figure 7a–c). Symptoms of HDM were observed from early spring and persisted throughout the growing season, ranging from moderate to severe intensity depending on the site and the phenological stage of the plants. Severe symptoms were recorded at Stekník during the period of intensive growth (BBCH 31) in early June and during the formation of reproductive organs (BBCH 71) at the end of July. At Nesuchyně, severe HDM symptoms were recorded at the end of July (BBCH 71) and in August (BBCH 89). At Tršice, moderate HDM symptoms were observed at BBCH 61.

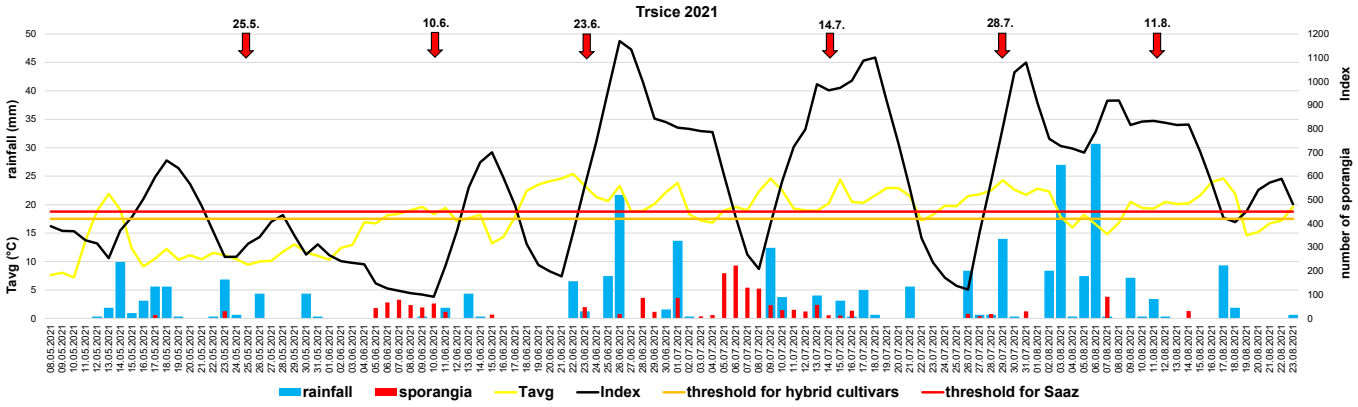


(**a**)



(**b**)

Figure 7. *Cont.*



(**c**)

Figure 7. Monitoring of *P. humuli* airborne sporangia using spore traps and qRT-PCR (red bars) in (**a**) Stekník, (**b**) Nesuchyně, and (**c**) Tršice in 2021. Daily average temperature (Tavg—yellow line) and daily rainfall (blue bars) were used for the calculation of the downy mildew prediction index (black line) for disease management. Thresholds for hybrid cultivars and the Saaz cultivar are shown in orange and red lines, respectively. Spraying dates are marked by arrows.

3.2.2. Airborne *P. humuli* Sporangia Occurrence During the 2022 Growing Season

In 2022, *P. humuli* sporangia were first detected using qPCR at both Stekník (Figure 8a) and Nesuchyně (Figure 8b) on 27 May. At Tršice, sporangia were first detected later, during the second week of June (8 June; Figure 8c). Sporangia of *P. humuli* continued to be detected at this site until the end of June, with a maximum on 9 June, except for the third week of June, the period from 26 to 28 June, and on 30 June, when no sporangia were recorded. During June, *P. humuli* sporangia were only sporadically detected at Stekník (Figure 8a), specifically on 12, 17, and 27 June. At Nesuchyně, *P. humuli* sporangia were recorded during the second week of June, peaking on 10 June, but no DNA was detected during the remainder of the month. In July, sporangia were sporadically detected at Stekník (Figure 8a) on 1, 2, 14, and 23 July. Toward the end of the growing season, a second pronounced period of DNA detection was observed at Stekník during the third week of August, with a maximum on 19 August. At Nesuchyně, *P. humuli* sporangia were subsequently detected at the transition between the second and third weeks of July, with the highest concentration recorded during the fourth week, specifically on 24 July. The last period of *P. humuli* sporangium occurrence at this site was observed during the third week of August. At Tršice, pathogen sporangia were detected only sporadically during the second week of July (on 8 and 10 July) and again at the end of the month (29 July). In August, detection was minimal, occurring only on 12 and 13 August. The course of the HDM weather index (I) corresponded closely with the pattern of selected meteorological parameters. Treatment applications (Figure 8a–c) in 2022 were timed by growers according to issued warning signals. Symptoms of HDM were first observed in Bohemia at the end of May and ranged from mild to moderate intensity at Stekník, where they were most pronounced at BBCH 89. At Nesuchyně, two major HDM waves were observed during BBCH 31–35 and again at BBCH 71–75. At Tršice, moderate HDM symptoms were recorded in June, corresponding to BBCH 31–39.

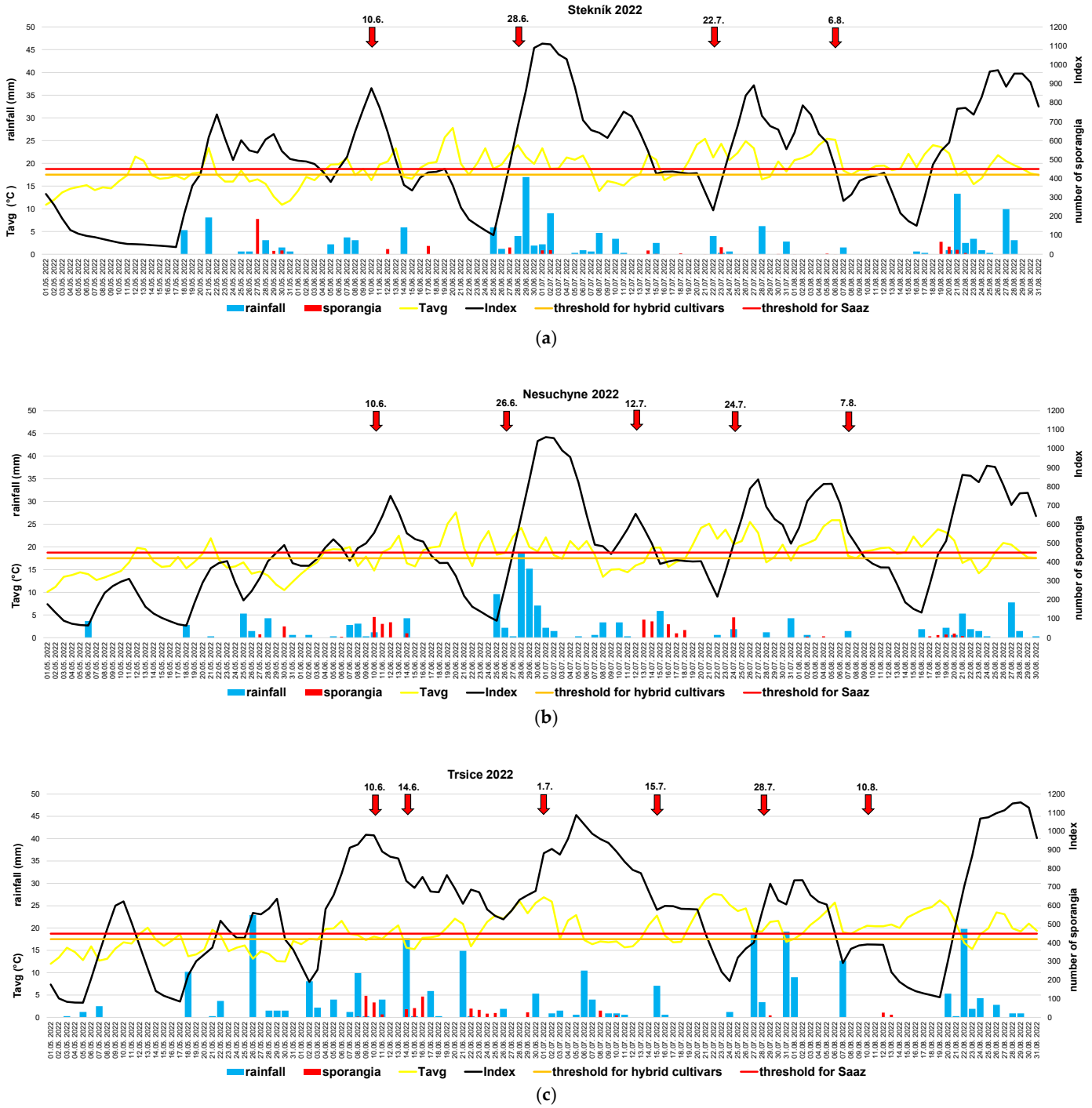


Figure 8. Monitoring of *P. humuli* airborne sporangia using spore traps and qRT-PCR (red bars) in (**a**) Steknik, (**b**) Nesuchyne, and (**c**) Trsice in 2022. Daily average temperature (Tavg—yellow line) and daily rainfall (blue bars) were used for calculation of the downy mildew prediction index (black line) for disease management. Thresholds for hybrid cultivars and the Saaz cultivar are shown in orange and red lines, respectively. Spraying dates are marked by arrows.

4. Discussion

The forecasting and timing of hop protection measures in Bohemian and Moravian growing regions are based on a modified short-term forecasting method for HDM. This approach relies on the calculation of the HDM weather index (I) and on the biological assessment of disease incidence in hop plants [5,6]. The current recommendations for initiating protective treatments are based on the assumption that the pathogen inoculum is

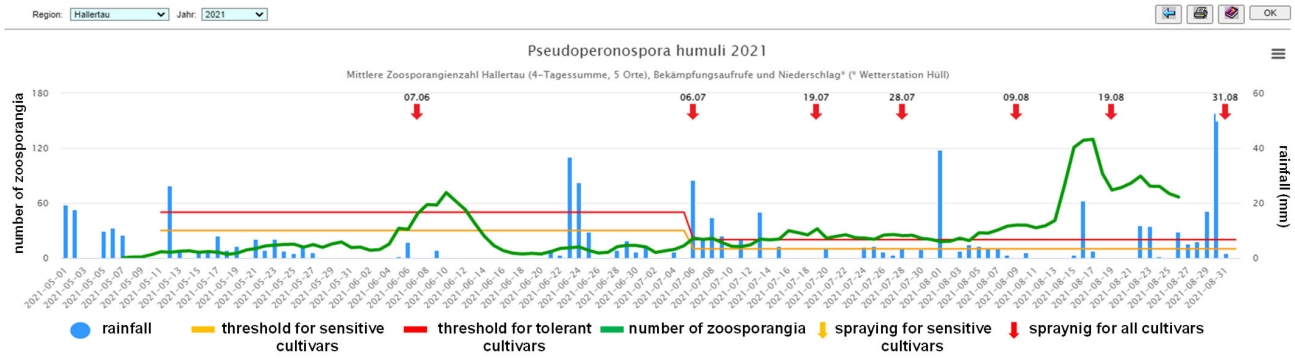
continuously present in the environment, since quantitative monitoring of zoosporangia density is not routinely performed under commercial conditions [10].

To monitor inoculum concentration, volumetric spore traps can be used; this methodology is employed in hop-growing regions of Germany to monitor the occurrence of zoosporangia [9]. However, the microscopic evaluation of collected samples is highly demanding and requires expert knowledge for distinguishing among sporulating pathogen species. For accurate species-specific detection and quantification of *P. humuli* sporangia captured by spore traps, the molecular qRT-PCR method can currently be employed [11–13,22,23]. Gent et al. [10] were the first to apply this detection approach, initially using a conventional PCR format targeting the ITS1 region of the rDNA sequence. This genomic region has been used for phylogenetic analyses together with the β-tubulin gene and the mitochondrial genes cytochrome c oxidase (*cox*2, *cox*2-1 spacer, and *cox*1) [16,18,24]. Phylogenetic analyses have demonstrated a high sequence similarity between *P. humuli* and *P. cubensis*. At the same time, they revealed a very low variability among *P. humuli* isolates, a finding further supported by subsequent sequencing studies [25,26]. These studies support the hypothesis of a clonal or highly inbred population structure in *P. humuli*, characterized by a homothallic mating system [27]. Species-specific PCR primers designed for *P. humuli* sequences detect all pathogen isolates occurring within individual sites. However, it is essential to identify non-homologous sequence regions between *P. humuli* and *P. cubensis* to avoid cross-amplification, as this was not possible for the qDMITS1 primer pair in our study, even with the internal BHQ1 probe. To discriminate sequences based on single-nucleotide polymorphisms (SNPs), high-resolution melting (HRM) analysis can be applied in qRT-PCR, as demonstrated by Lee et al. [23] for the β-tubulin gene and by Summers et al. [22] for the mitochondrial *cox2* gene. For SNP analysis in the *cox2* gene locus, locked nucleic acid (LNA) probes can also be used [22], as demonstrated by Bello et al. [12], who successfully employed them for the quantification of sporangia collected from volumetric spore traps. A certain limitation of this approach is the high copy number of the target mitochondrial sequence within individual cells, which may vary from cell to cell, thereby reducing the accuracy of sporangium quantification. Nevertheless, Crandall et al. [11] used the mitochondrial ORF329 sequence for the quantification of sporangium suspensions using qRT-PCR with TaqMan probes. Although a certain degree of variability was observed—likely due to the extraction of very small amounts of DNA from individual sporangia—the cells were in similar developmental stages, resulting in relatively uniform mitochondrial content compared to mycelial cells at various developmental phases. Therefore, for more accurate quantification, it is preferable to target nuclear genomic DNA sequences that are specific to *P. humuli* and absent from the *P. cubensis* genome. Rahman et al. [17] identified four such sequences: c125015.3e1, c127446.1e1, c127233.5e3, and c126365.1e5. In our study, three of these sequences were tested using qRT-PCR, with c127233.5e3 (qPhu2) showing the best performance. Higgins et al. [13] also examined these sequences but were unable to design suitable PCR primers for c127233.5e3. Primers designed for c126365.1e5 (qPhu3) exhibited a high level of homology with other species in the NCBI GenBank database https://blast.ncbi.nlm.nih.gov/Blast.cgi (accessed on 30 December 2025) and potential off-target binding sites. Consequently, the sequence c125015.3e1 (not used in our study) was selected for a qRT-PCR assay with internal BHQ1 probes. The mitochondrial sequence ORF359 was also employed to test infection in various hop tissues. The obtained results confirmed that the mitochondrial sequence was amplified more strongly and exhibited higher variability in quantification values among the sporangium samples. These findings clearly support the use of our qPhu2 qRT-PCR assay with internal BHQ1 probes for the detection of *P. humuli* sporangia from volumetric spore trap samples.

The epidemiological conditions during 2021 and 2022 differed markedly. The year 2021 provided optimal conditions for the development of HDM. Precipitation was evenly distributed, while high relative humidity and average temperatures around 20 °C likely promoted both pathogen reproduction and infection activity. From May to August 2021, significant concentrations of sporangia were detected at all monitored sites, showing distinct peak periods that coincided with critical phenological stages depending on the location. The high infection potential of the pathogen was also reflected in the elevated HDM weather index (I) values, which remained above the threshold of harmfulness for most of the season. The higher sporangium counts and DNA detection rates of *P. humuli* observed in 2021 corresponded to prolonged periods of humidity that favor sporulation, whereas short-term intensive rainfall events may have washed sporangia off the plant surfaces [28,29]. This is supported by the low sporangium counts recorded after single rainfall events exceeding 25 mm. The relatively cool and rainy spring of 2021 likely delayed plant growth, which may have increased susceptibility to infection. Since *P. humuli* overwinters in dormant hop crowns and buds, from which basal shoots emerge in spring and early summer [30], the onset of infection is strongly dependent on favorable meteorological conditions. In the absence of a specific control strategy targeting primary infection, preventive treatments or interventions at the appearance of primary shoots are essential, and their proper timing is critical to reduce the pathogen's inoculum potential and limit the development of secondary infections [31]. At all monitored sites, higher sporangium concentrations were associated with rainfall periods and correlated with disease severity. Growers applied treatments according to issued warning signals, regardless of the actual sporangium occurrence. The only limiting factor was exceptionally high rainfall, which prevented optimal-timing applications at the Stekník site. The year 2022 was characterized by warmer and drier conditions. Detection of pathogen DNA was considerably lower throughout the monitoring period compared with the previous year, resulting in reduced infection pressure. Symptoms of HDM were observed at the Bohemian sites only at the end of May, when the pressure of primary infection was strongly limited by the nature of the spring weather. At Tršice, the first symptoms were recorded even later, at the beginning of June. These observations confirm that the development of infection is closely associated with weather patterns, consistent with the polyetic nature of the disease. Detection of *P. humuli* sporangia, as in the previous year, was significant mainly after rainfall events, and the HDM weather index (I) also reached its maximum values during these periods. In contrast, sporangium detection was sporadic during dry intervals. This finding supports the observations of Royle and Thomas [29], who reported that sporangia lose their ability to germinate after 12–18 h of dry conditions. Although the HDM weather index (I) frequently reached high values and rarely dropped below the threshold of harmfulness during the vegetation period, *P. humuli* sporangia were not detected at the same levels as in 2021. The low sporangium count may be partly explained by the limited vertical range of the spore traps, which might not fully reflect the actual inoculum load within the crop canopy. In addition, it can be assumed that preventive fungicide treatments applied according to warning signals contributed to a reduction in the number of airborne sporangia. Based on our observations in 2021 and 2022, it can be stated that the release of sporangia occurs after a period of sustained tissue wetness, following higher precipitation totals and temperatures oscillating around 20 °C, which corresponds to the same findings as those reported by Gent and Ocamb [32]. This concurrence of selected variables indicates that the HDM weather index (I) adequately reflected the epidemiological potential of the pathogen and the actual presence of inoculum in the environment. The findings suggest that an increase in the number of sporangia was recorded with a delay of 1–2 weeks after the period during which the treatment recommendation was issued. This observation correlates with the biological cycle

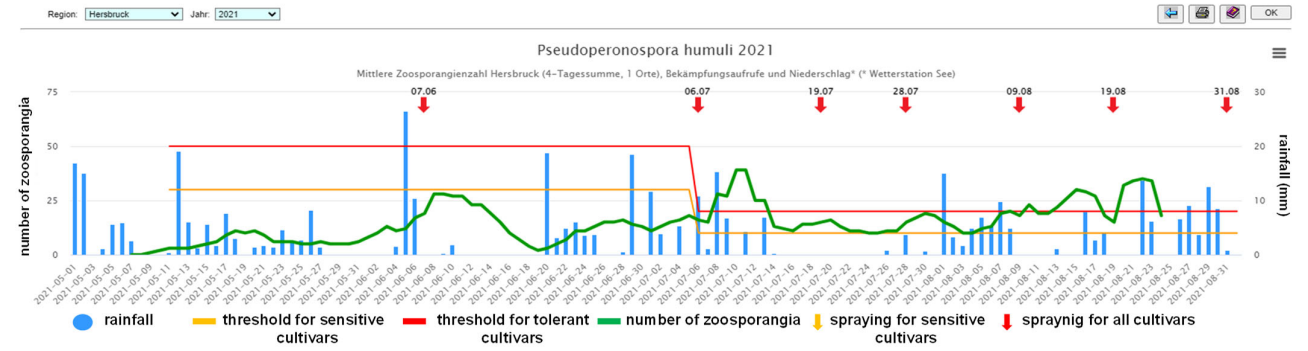
of the pathogen, as it requires a certain amount of time for the development of sporangia on the sporangiophores, which occurs only after the microclimatic conditions optimal for their maturation have stabilized. The observed temporal sequence can be explained by the fact that the HDM weather index (I) detects infection conditions for mycelial growth and sporangiophore differentiation, whereas the release of the sporangia themselves represents a subsequent phase of the pathogen's reproductive cycle, which can be monitored using volumetric spore traps. Therefore, the treatment-warning system currently used in the CR can be considered appropriate based on our findings, since correct timing of fungicide application should precede the sporulation phase.

In comparison, the German model (Bayerische Landesanstalt für Landwirtschaft) (Figures 9 and 10) uses data on the concentration of zoosporangia in the air as an early warning system for growers, signaling the likely occurrence of HDM and prompting treatment. A potential issue with this is that evaluation by light microscopy may lead to the misidentification of species within the genus *Pseudoperonospora*, and specifically, confusion with *P. cubensis*, as indicated by Bello et al. [15]. A comparison of both approaches shows that in the German system, the recommended treatment date corresponds to the sporulation phase, whereas the Czech system targets the intervention preventively, thereby providing more time for the effective suppression of infections. However, the absence of direct information about the presence of inoculum may lead to a temporal mismatch between prediction and actual infection pressure. The results obtained in Germany for 2021 correlated with the data measured in the CR, where the first peak in zoosporangium quantity appeared at all locations at the beginning of June (Figure 9a–c). Overall, the number of zoosporangia remained high, with peaks occurring at the beginning of July at the Hersbruck site (Figure 9b), similar to the Tršice site (Figure 7c); at the end of July at the Spalt site (Figure 9c), similar to the Stekník and Nesuchyně sites (Figure 7a,b); and in mid-August at the Hallertau and Hersbruck sites (Figure 9a,b), as observed at the Nesuchyně site (Figure 7b). In 2022, the number of zoosporangia remained at a low level (Figure 10a–c), corresponding to low infection pressure, similar to the situation in the CR (Figure 8a–c). Significant peaks at the beginning, in the middle, and at the end of June at all monitored locations were similar to the infection dynamics at the Tršice site (Figure 8c). At the Nesuchyně site, an increased occurrence of spores also appeared at the beginning of June and then in mid-July (Figure 8b). This slightly elevated occurrence was recorded in Germany only at the Hallertau site (Figure 10a). These results confirm that qRT-PCR is fully comparable to light microscopy.

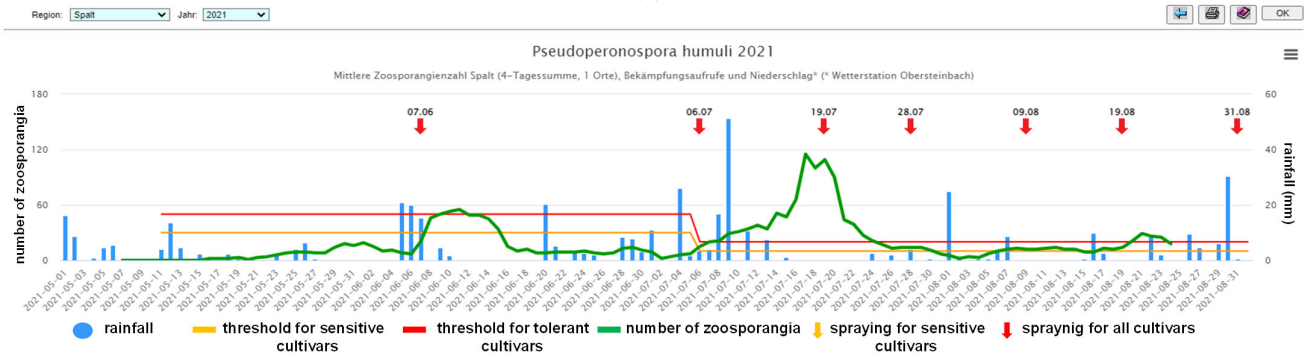


(**a**)

Figure 9. *Cont.*



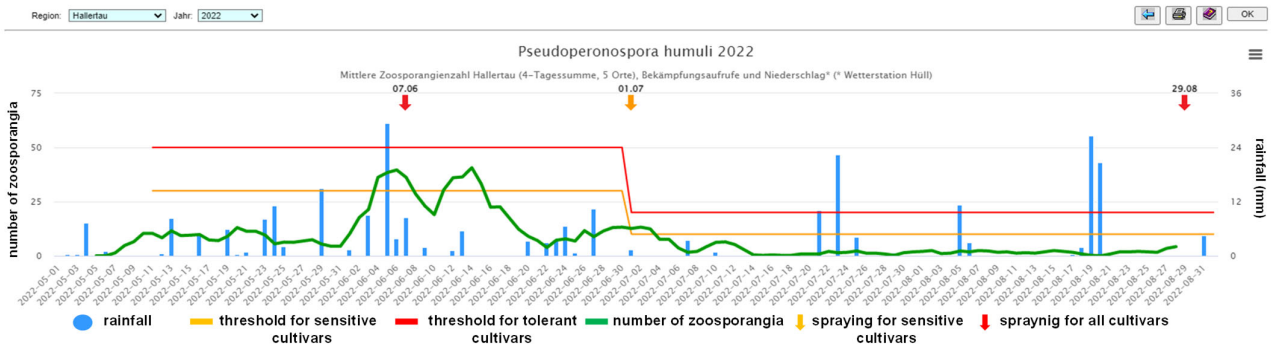
(**b**)



(**c**)

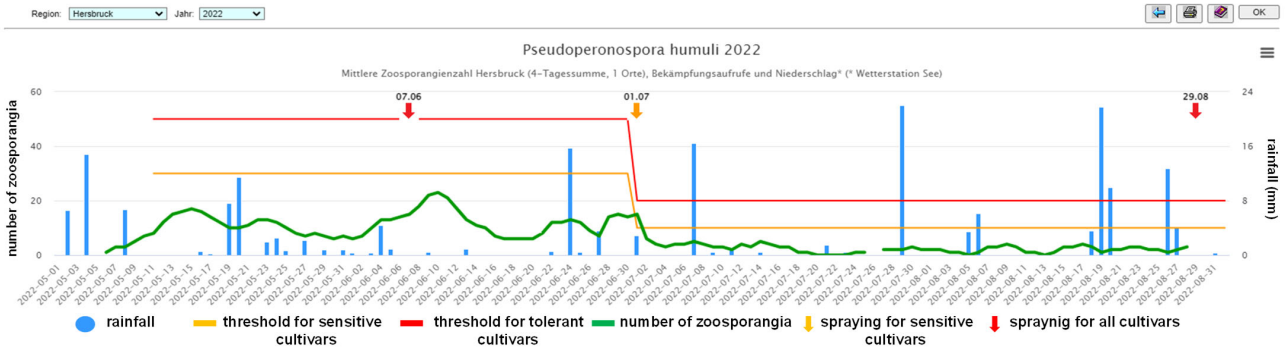
Figure 9. Monitoring of *P. humuli* zoosporangia using spore traps and light microscopy counting (green line) in (**a**) Hallertau, (**b**) Hersbruck, and (**c**) Spalt in 2021. Daily rainfall (blue bars) and zoosporangium thresholds for sensitive (orange line) and tolerant (red line) hop cultivars are shown on the plot. Warning recommendations for spraying are marked by arrows https://www.wetter-by.de/Agrarmeteorologie-BY/Landwirtschaft/Hopfen/Peronospora-Monitoring (accessed on 21 October 2025).

The results obtained also confirm that the combination of spore traps and qRT-PCR can significantly improve the accuracy of short-term forecasting systems and contribute to a better understanding of the spread dynamics of *P. humuli*. Although molecular methods demonstrate high sensitivity and enable early detection of infection pressure, their practical implementation under Czech conditions faces technical and economic limitations. Hop cultivation occupies a relatively small area (compared with other crops), and the costs of regular PCR diagnostics under commercial conditions would be disproportionate given the scale of production. In line with this assertion, Bello et al. [15] note that although the accuracy of molecular detection is high, its operational application requires substantial infrastructure, which may not always be available in practice.

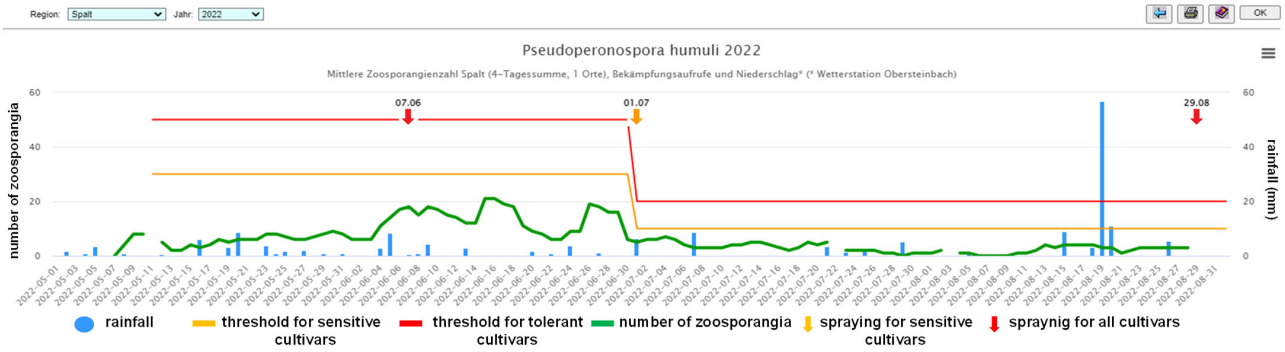


(**a**)

Figure 10. *Cont.*



(**b**)



(**c**)

Figure 10. Monitoring of *P. humuli* zoosporangia using spore traps and light microscopy counting (green line) in (**a**) Hallertau, (**b**) Hersbruck, and (**c**) Spalt in 2022. Daily rainfall (blue bars) and zoosporangium thresholds for sensitive (orange line) and tolerant (red line) hop cultivars are shown on the plot. Warning recommendations for spraying are marked by arrows https://www.wetter-by.de/Agrarmeteorologie-BY/Landwirtschaft/Hopfen/Peronospora-Monitoring (accessed on 21 October 2025).

5. Conclusions

Based on our results, we recommend using spore traps in representative locations (with a high risk of infection) and adjusting the current threshold value of HDM weather index (I), or shortening the interval between applications, during the period of fructification. Such an approach may better account for interannual variability. Modern diagnostic methods have a firmly established place within plant protection systems, particularly at a time when emphasis is placed on reducing the number of active substances and on the rational use of fungicides. This approach can slow the development of pathogen resistance while simultaneously reducing the costs of protecting against *P. humuli*.

Author Contributions: Conceptualization, M.T. and J.P.; methodology, M.T., A.H., J.P. and I.K.; software, J.P.; supervision, I.K. and J.P.; investigation, M.T., I.K. and J.P.; writing—original draft preparation, M.T. and J.P.; writing—review and editing, M.T., I.K. and J.P.; English language and style, M.T.; visualization, J.P. and M.T.; funding acquisition, J.P. All authors have read and agreed to the published version of the manuscript.

Funding: This work was supported by the Ministry of Agriculture of the Czech Republic within Institutional Support MZe-RO1325.

Data Availability Statement: The original contributions presented in this study are included in the article. Further inquiries can be directed to the corresponding author.

Acknowledgments: The authors want to thank the local hop growers for providing part of their hop gardens to conduct this field trial.

Conflicts of Interest: Authors Markéta Trefilová, Ivo Klapal, Alena Henychová and Josef Patzak were employed by the Hop Research Institute Co., Ltd. The remaining authors declare that the research was conducted in the absence of any commercial or financial relationships that could be construed as a potential conflict of interest.

Abbreviations

The following abbreviations are used in this manuscript:

qRT-PCR	quantitative Real-Time PCR
HDM	Hop Downy Mildew
CR	Czech Republic
DNA	Deoxyribonucleic Acid
rDNA	Ribosomal DNA
SNPs	Single-Nucleotide Polymorphisms
LNA	Locked Nucleic Acid
HRM	High-Resolution Melting Analysis
NCBI	National Center for Biotechnology Information

References

1. Natsume, S.; Takagi, H.; Shiraishi, A.; Murata, J.; Toyonaga, H.; Patzak, J.; Takagi, M.; Yaegashi, H.; Uemura, A.; Mitsuoka, C.; et al. The draft genome of hop (*Humulus lupulus*), an essence for brewing. *Plant Cell Physiol.* **2015**, *56*, 428–441. [CrossRef]
2. Sakamoto, K.; Konings, W.N. Beer spoilage bacteria and hop resistance. *Int. J. Food Microbiol.* **2003**, *89*, 105–124. [CrossRef]
3. Gent, D.H. Downy mildew. In *Field Guide for Integrated Pest Management in Hops*; O'Neal, S.D., Walsh, D.B., Gent, D.H., Eds.; Hop Industry Plant Protection Committee: Pullman, WA, USA, 2015; pp. 15–21. ISBN 978-0890543764.
4. Royle, D.J.; Kremheller, H.T. Downy mildew of the hop. In *The Downy Mildews*; Spencer, D.M., Ed.; Academic Press: New York, NY, USA, 1981; pp. 395–419, ISBN 978-0126568608.
5. Krofta, K.; Jezek, J.; Klapal, I.; Krivánek, J.; Pokorný, J.; Pulkrábek, J.; Vostrel, J. Integrated systém for hop cultivation. In *Methodology for Praxis 2/2012*; Hop Research Institute Co., Ltd.: Zatec, Czech Republic, 2012; 85p, ISBN 978-80-86836-82-9. (In Czech)
6. Gent, D.H.; Nelson, M.E.; Farnsworth, J.L.; Ocamb, C.M.; Grove, G.G. Systems approaches to mangement of hop downy mildew. In *Proceedings of the Scientific Commission of I.H.G.C., Spain, León, 21–25 June 2009*; Seigner, E., Ed.; Hop Research Center Hüll: Wolnzach, Germany, 2009; pp. 80–83, ISSN 1814-2206.
7. Engelhard, B.; Schlagenhaufer, S. A forecasting model for the control of powdery mildew (*Podosphaera macularis*) in hops (*Humulus lupulus*) under climatic conditions in the Hallertau. In *Proceedings of the Scientific Commission of I.H.G.C., Spain, León, 21–25 June 2009*; Seigner, E., Ed.; Hop Research Center Hüll: Wolnzach, Germany, 2009; pp. 77–79, ISSN 1814-2206.
8. Hirst, J.M. An automatic volumetric spore-trap. *Ann. App. Biol.* **1952**, *36*, 257–265. [CrossRef]
9. Portner, J. 50% plant protection product savings thanks to the downy mildew warning service. *Hopfen-Rundsch. Int. 2021/2022* **2021**, 109–115. Available online: https://tettnanger-hopfen.de/aktuelles/detail/news/hopfen-rundschau-international-2021-2022/?utm_source=chatgpt.com (accessed on 11 February 2026).
10. Gent, D.H.; Nelson, M.E.; Farnsworth, J.L.; Grove, G.G. PCR detection of *Pseudoperonospora humuli* in air samples from hop yards. *Plant Pathol.* **2009**, *58*, 1081–1091. [CrossRef]
11. Crandall, S.G.; Ramon, M.L.; Burkhardt, A.K.; Bello Rodriguez, J.C.; Adair, N.; Gent, D.H.; Hausbeck, M.K.; Quesada-Ocampo, L.M.; Martin, F.N. A Multiplex TaqMan qPCR assay for detection and quantification of Clade 1 and Clade 2 isolates of *Pseudoperonospora cubensis* and *Pseudoperonospora humuli*. *Plant Dis.* **2021**, *105*, 3154–3161. [CrossRef]
12. Bello, J.C.; Sakalidis, M.L.; Perla, D.E.; Hausbeck, M.K. Detection of airborne sporangia of *Pseudoperonospora cubensis* and *P. humuli* in Michigan using Burkard spore traps coupled to quantitative PCR. *Plant Dis.* **2021**, *105*, 1373–1381. [CrossRef] [PubMed]
13. Higgins, D.S.; Miles, T.D.; Byrne, J.M.; Hausbeck, M.K. Optimizing molecular detection for the Hop Downy Mildew pathogen *Pseudoperonospora humuli* in plant tissue. *Phytopathology* **2022**, *112*, 2426–2439. [CrossRef]
14. EPPO Standard. PP 1/003 (4): *Pseudoperonospora humuli*. *EPPO Bull.* **2013**, *43*, 9–11.
15. Hospodsky, D.; Yamamoto, N.; Peccia, J. Accuracy, precision, and method detection limits of quantitative PCR for airborne bacteria and fungi. *Appl. Environ. Microbiol.* **2010**, *76*, 7004–7012. [CrossRef]
16. Werschallová, M.; Patzak, J.; Henychová, A. Molecular genetic analysis of *Pseudoperonospora humuli* populations in hop growing areas in the Czech Republic. *Acta Hortic.* **2021**, *1328*, 55–62. [CrossRef]

17. Rahman, A.; Góngora-Castillo, E.; Bowman, M.J.; Childs, K.L.; Gent, D.H.; Martin, F.N.; Quesada-Ocampo, L.M. Genome sequencing and transcriptome analysis of the Hop Downy Mildew pathogen *Pseudoperonospora humuli* reveal species-specific genes for molecular detection. *Phytopathology* **2019**, *109*, 1354–1366. [CrossRef]
18. Runge, F.; Choi, Y.-J.; Thines, M. Phylogenetic investigations in the genus *Pseudoperonospora* reveal overlooked species and cryptic diversity in the *P. cubensis* species cluster. *Eur. J. Plant Pathol.* **2011**, *129*, 135–146. [CrossRef]
19. Lee, D.J.; Lee, J.S.; Choi, Y.J. Co-Occurrence of two phylogenetic clades of *Pseudoperonospora cubensis*, the causal agent of downy mildew disease, on oriental pickling melon. *Mycobiology* **2021**, *49*, 188–195. [CrossRef] [PubMed]
20. EPPO Standard. PM 7/98 (5) Specific requirements for laboratories preparing accreditation for a plant pest diagnostic activity. *EPPO Bull.* **2021**, *51*, 468–498. [CrossRef]
21. Krofta, K.; Mravcová, L.; Kolek, D.; Patáková, P.; Patzak, J.; Henychová, A.; Dostálek, P. Microbial community of hop (*Humulus lupulus* L.) and its impact on the quality of hop products. *Acta Hortic.* **2021**, *1328*, 109–114. [CrossRef]
22. Summers, C.F.; Adair, N.L.; Gent, D.H.; McGrath, M.T.; Smart, C.D. *Pseudoperonospora cubensis* and *P. humuli* detection using species-specific probes and high definition melt curve analysis. *Can. J. Plant Pathol.* **2015**, *37*, 315–330. [CrossRef]
23. Lee, J.H.; Park, M.H.; Lee, S. Identification of *Pseudoperonospora cubensis* using real-time PCR and high resolution melting (HRM) analysis. *J. Gen. Plant Pathol.* **2016**, *82*, 110–115. [CrossRef]
24. Mitchell, M.N.; Ocamb, C.M.; Grünwald, N.J.; Mancino, L.E.; Gent, D.H. Genetic and pathogenic relatedness of *Pseudoperonospora cubensis* and *P. humuli*. *Phytopathology* **2011**, *101*, 805–818. [CrossRef]
25. Gent, D.H.; Adair, N.; Knaus, B.J.; Grünwald, N.J. Genotyping-by-Sequencing reveals fine-scale differentiation in populations of *Pseudoperonospora humuli*. *Phytopathology* **2019**, *109*, 1801–1810. [CrossRef]
26. Kitner, M.; Runge, F.; Lebeda, A.; Vaculná, L.; Sedláková, B.; Thines, M. *Pseudoperonospora humuli* might be an introduced species in Central Europe with low genetic diversity but high distribution potential. *Eur. J. Plant Pathol.* **2021**, *159*, 903–915. [CrossRef]
27. Gent, D.H.; Cohen, Y.; Runge, F. Homothallism in *Pseudoperonospora humuli*. *Plant Pathol.* **2017**, *66*, 1508–1516. [CrossRef]
28. Gent, D.H.; Ocamb, C.M.; Farnsworth, J.L. Forecasting and management of hop downy mildew. *Plant Dis.* **2010**, *94*, 425–431. [CrossRef] [PubMed]
29. Royle, D.J.; Thomas, G.P. Epidemiology of downy mildew (*Pseudoperonospora humuli*) on hops (*Humulus lupulus* L.). *Ann. Appl. Biol.* **1971**, *67*, 289–306.
30. Coley-Smith, J.R. Overwintering of *Pseudoperonospora humuli* in dormant hop buds. *Trans. Br. Mycol. Soc.* **1962**, *45*, 253–260.
31. Richardson, B.J.; Gent, D.H. Impact of infection timing and autumnal fungicide applications on perennation of *Pseudoperonospora humuli* and severity of hop downy mildew. *Plant Dis.* **2023**, *107*, 3430–3436. [CrossRef]
32. Gent, D.H.; Ocamb, C.M. Predicting infection risk of hop by *Pseudoperonospora humuli*. *Phytopathology* **2009**, *99*, 1190–1198. [CrossRef] [PubMed]

Disclaimer/Publisher's Note: The statements, opinions and data contained in all publications are solely those of the individual author(s) and contributor(s) and not of MDPI and/or the editor(s). MDPI and/or the editor(s) disclaim responsibility for any injury to people or property resulting from any ideas, methods, instructions or products referred to in the content.